Soliman *Beni-Suef Univ J Basic Appl Sci* (2022) 11:81
https://doi.org/10.1186/s43088-022-00261-9

Beni-Suef University Journal of Basic and Applied Sciences

RESEARCH Open Access

Radiative MHD flow of Rivlin–Ericksen nanofluid of grade three through porous medium with uniform heat source

Hussein Abd Allah Soliman*

Abstract

Background: The paper investigates the analytical and numerical solution of the radiation effect on MHD flow of Rivlin–Ericksen nanofluid of grade three through a porous medium with a uniform heat source between two vertical flat plates. The governing equations are solved analytically using multi-step differential transform method (MDTM) and numerically using finite difference method (FDM) and shooting method by designing MATLAB and Mathematica algorithms. The study discovered that the MDTM, FDM, and shooting methods are effective for solving nonlinear differential equations like this one.

Results: Graphs and tables show the influence of different parameters on velocity and temperature. Figures and tables show the comparisons between current outcomes and previous results that are accessible.

Conclusions: The present results showed that the analytical and numerical solutions agree well with previously published outcomes.

Keywords: Rivlin–Ericksen nanofluid, Radiation, Magnetic field, Porous medium, Heat source, Analytical and numerical solutions

1 Background

The analysis of heat transfer characteristics of various fluid flows can be extremely useful in improving the performance of industrial systems. Natural convection can highly be significant, especially when moving fluid is minimally influenced by forced convection heat transfer. Natural convection has piqued the interest of scientists since it occurs in a variety of technical applications. Geothermal systems, heat exchangers, chemical catalytic reactors, fiber and granular insulation, packed beds, petroleum reservoirs, and nuclear waste dumps all use natural convection to transfer heat [1–3]. Mixed convection of Cu–water nanofluid inside a two-sided lid-driven cavity filled with heterogeneous porous media is optimized. The horizontal walls are adiabatic and movable, and the vertical walls are exposed to constant hot and cold temperatures. Two-phase mixture model and Darcy–Brinkman–Forchheimer relation are implemented, respectively, for the simulation of nanofluid and fluid flow through porous media [4–6]. In the recent decade, various researchers investigated exergy analyses and entropy generation to provide the best geometry of the heat exchanger. Using nanofluid and swirl flow devices are passive techniques for improving thermal efficiency. Exergy variations for forced convection of nanofluid through a pipe equipped with twisted tape turbulators have been simulated via finite volume method [7, 8].

The study of blood flow through a stenosed artery is very important because of the fact that the cause and development of many cardiovascular diseases are related to the nature of blood movement and the mechanical behavior of the blood vessel walls. Stenosis is defined as a partial occlusion of the blood vessels due to the

*Correspondence: Hussein.AbdAllah.Soliman@iaems.edu.eg

Engineering Division, Department of Basic Science, International Academy for Engineering and Media Science, 6th October, Egypt

accumulation of cholesterol, fats, and the abnormal growth of tissue. Cardiac catheterization (also called heart catheterization) is a diagnostic procedure that does a comprehensive examination to determine how the heart and its blood vessels function. One or more catheter is inserted through a peripheral blood vessel in the arm (antecubital artery or vein) or leg (femoral artery or vein) with X-ray guidance. This procedure gathers information such as adequacy of blood supply through the coronary arteries, blood pressure, blood flow throughout chambers of the heart, collection of blood samples, and X-rays of the heart's ventricles or arteries [9, 10].

Analysis of natural convection is often difficult, particularly when a non-Newtonian fluid is flowing in a system. Various flows of Newtonian and non-Newtonian fluids bounded by two infinite parallel vertical plates have been studied analytically, numerically, and experimentally by numerous scholars. A numerical solution is investigated for Rivlin–Ericksen fluid natural convection flow and heat transfer between parallel plates. Nowadays, much attention is being paid to the application of nanofluids for cooling purposes [11–13].

Nanoparticles can significantly improve the thermal conductivity of base fluids by altering their thermophysical properties, resulting in improved heat transfer [14–17]. Chamkha [18], using continuum equations, constructed a mathematical model for a continuous two-phase non-Newtonian fluid flow over an infinite porous flat plate. Ellahi et al. [19] used series solutions to investigate the heat transfer features of a fully developed incompressible non-Newtonian fluid flow in coaxial cylinders using Reynolds and Vogel models. Youssri et al. [20, 21] presented a numerical technique for solving one- and two-dimensional partial differential heat equation and the fractional Bagley–Torvik equation with homogeneous boundary conditions by employing the tau and collocation methods. The Runge–Kutta method was used to investigate the influence of free convection flow on non-Newtonian fluid flow through a porous media along with an isothermal vertical flat plate [22]. The natural convection of a non-Newtonian nanofluid flow between two infinite parallel vertical flat plates was investigated analytically using the differential transformation approach. Domairry et al. [23] discovered that as the volume percentage of nanoparticles grows, the thickness of the momentum boundary layer increases while the thickness of the thermal boundary layer drops.

Pittman et al. [24] examined the natural convection heat transfer of a non-Newtonian fluid moving over an electrically heated vertical plate under constant surface heat flux circumstances and found that the temperature difference grows as the distance between the fluid and the plate increases. Using analytical and numerical approaches, Hatami et al. [25] examined the natural convection of a non-Newtonian nanofluid flow between two vertical flat plates. The Boussinesq approach was utilized by Ternik et al. [26] to calculate the natural convection of non-Newtonian nanofluids in a square differentially heated chamber.

The aim of this work is to investigate analytical and numerical solutions of the radiation effect on MHD flow of Rivlin–Ericksen nanofluid of grade three through porous medium with uniform heat source between two vertical flat plates. In addition, the effects of dimensionless non-Newtonian viscosity, radiation, porosity parameter, Hartmann number, Eckert number, Prandtl number, and heat source parameter on the temperature and velocity of flow between two infinitely parallel vertical flat plates are investigated. The reduced ordinary differential equations are solved using MDTM, FDM, and shooting method. This approach provides highly accurate solution estimates in a series of steps. The variation distribution of velocity and temperature with the parameters that govern the problem is presented. Furthermore, graphical and numerical results for the velocity and temperature profiles are presented and discussed for various parametric conditions. Finally, comparisons with previously published works are made and showed that the present results have high accuracy and are found to be in good agreement.

2 Mathematical formulation of the problem

A schematic of the problem under study is shown in Fig. 1. It consists of two flat plates that can be positioned vertically. A non-Newtonian fluid is contained on two flat plates separated by $2b$. At $x = +\mathrm{b}$ and $x = \mathrm{b}$, the walls are kept at constant temperatures T_1 and T_2, respectively, with $T_1 > T_2$. The fluid near the wall is caused by the temperature difference, at $x = -b$ to rise and at $x = +b$ to fall [27]. The fluid is a water-based nanofluid containing copper. The base

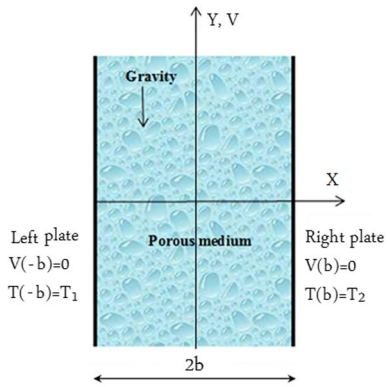

Fig. 1 Schematic diagram of the problem under investigation

fluid and the nanoparticles are considered to be in thermal equilibrium, with no slide between them. Table 1 lists the nanofluid's thermophysical properties [28].

Radiative heat flux q_r can be calculated by using Rosseland approximation as follows [29, 30]:

$$q_r = -\frac{4\sigma^*}{3k^*}\frac{\partial T^4}{\partial x}, \tag{1}$$

where the Stephan–Boltzmann constant and the mean absorption coefficient, respectively, are represented by σ^* and K^*. The temperature differences in the flow are supposed to vary by the fourth power of T which can be expressed by a linear function of temperature. This can be implemented by expansion of T^4 based on Taylor series as follows [29]:

$$T^4 = T_\infty^4 + 4T_\infty^3(T - T_\infty) + 6T_\infty^2(T - T_\infty)^2 + \cdots \tag{2}$$

By neglecting higher-order terms of temperature in Eq. (2) against the first-degree term, the following expression is achieved [29]:

$$\left(T^4 \cong 4T_\infty^3 T - 3T_\infty^4\right) \tag{3}$$

Subsequently, by substituting Eq. (3) into Eq. (1), radiative heat flux is rewritten as follows [29]:

$$q_r = -\frac{16\,T_\infty^3\sigma^*}{3k^*}\frac{\partial T}{\partial x} \tag{4}$$

The effective density ρ_{nf}, the effective dynamic viscosity μ_{nf}, the heat capacitance $(\rho C_p)_{nf}$, and the thermal conductivity κ_{nf} of the nanofluid can be expressed by the solid volume fraction φ as

$$\rho_{nf} = \rho_f(1-\varphi) + \rho_f\varphi \tag{5}$$

$$\mu_{nf} = \frac{\mu_f}{(1-\varphi)^{2.5}} \tag{6}$$

$$(\rho C_p)_{nf} = (\rho C_p)_f(1-\varphi) + (\rho C_p)_s\varphi \tag{7}$$

$$\frac{\kappa_{nf}}{\kappa_f} = \frac{\kappa_s + 2\kappa_f - 2\varphi(\kappa_f - \kappa_s)}{\kappa_s + 2\kappa_f + \varphi(\kappa_f - \kappa_s)} \tag{8}$$

Table 1 Thermo-physical properties of water and nanoparticles

Material	Density (ρ) (kg/m^3)	C_p (J/Kg.k)	K (w/m.k)	$\beta \times 10^5$ (k^{-1})
Pure water	997.1	4179	0.613	21
Copper	8933	385	401	1.67

$$\frac{\sigma_{nf}}{\sigma_f} = 1 + \frac{3\left(\frac{\sigma_s}{\sigma_f} - 1\right)\varphi}{\left(\frac{\sigma_s}{\sigma_f} + 2\right) - \left(\frac{\sigma_s}{\sigma_f} - 1\right)} \tag{9}$$

The Navier–Stokes and energy equations can be constructed as follows under these assumptions and using the nanofluid model presented by Maxwell Garnett (MG) model [31]:

The equation of motion is [32 and 31]:

$$\mu_{nf}\frac{d^2u}{dx^2} + 6\beta_3\left(\frac{du}{dx}\right)^2\frac{d^2u}{dx^2} + \rho_o\gamma(T - T_m)g - \frac{\mu_{nf}}{K_{nf}}u - \sigma_{nf}\beta_0^2 u = 0, \tag{10}$$

and the energy equation is as follows:

$$K_{nf}\frac{d^2T}{dx^2} + 2\beta_3\left(\frac{du}{dx}\right)^4 + \mu_{nf}\left(\frac{du}{dx}\right)^2 + Q_0(T - T_m) - \frac{dq_r}{dx} = 0, \tag{11}$$

Rajagopal [27] has demonstrated that by using the similarity variables:

$$v = \frac{u}{u_0},\ \eta = \frac{x}{b} \text{ and } \theta = \frac{T - T_m}{T_1 - T_2}, \tag{12}$$

By substituting the above parameters, the Navier–Stokes equations and the energy equations can be reduced to two ordinary differential equations:

$$\frac{d^2v}{d\eta^2} + 6\delta(1-\varphi)^{2.5}\left(\frac{dv}{d\eta}\right)^2\frac{d^2v}{d\eta^2} + \theta - A\mathrm{Ha}^2(1-\varphi)^{2.5}v - \frac{P}{B}v = 0, \tag{13}$$

$$\left(1 + \frac{4}{3BR_d}\right)\frac{d^2\theta}{d\eta^2} + 2\delta\ \mathrm{Ec}\ \mathrm{Pr}\left(\frac{dv}{d\eta}\right)^4 + \left(\frac{\mathrm{Ec}\ \mathrm{Pr}}{B}\right)(1-\varphi)^{-2.5}\left(\frac{dv}{d\eta}\right)^2 + \frac{\alpha}{B}\theta = 0, \tag{14}$$

where $A = \frac{\sigma_{nf}}{\sigma_f}$, $B = \frac{\kappa_{nf}}{\kappa_f}$, $\mu_{nf} = \frac{\mu_f}{(1-\varphi)^{2.5}}$, $\nu_o = \frac{\rho_0\gamma g b^2(T_1 - T_2)}{\mu_{nf}}$, $\delta = \frac{\beta_3 u_0^2}{\mu_f b^2}$ is the dimensionless non-Newtonian viscosity, $P = \frac{b^2}{k_f}$ is the porosity parameter, $\mathrm{Ha}^2 = \frac{\sigma_f\beta_0^2 b^2}{\mu_f}$ is the Hartmann number, $R_d = \frac{kk^*}{4\sigma^* T_\infty^3}$ is the radiation parameter, $\mathrm{Ec} = \frac{u_0^2}{c_f(T_1 - T_2)}$ is the Eckert number, $\mathrm{Pr} = \frac{\mu_f c_f}{k_f}$ is the Prandtl number and $\alpha = \frac{Q_0 b^2}{k_f}$ is the heat source parameter.

The following are the appropriate boundary conditions:

$$v(-1) = 0,\ \theta(-1) = \frac{1}{2}, \tag{15}$$

$$v(1) = 0,\ \theta(1) = -\frac{1}{2}, \tag{16}$$

3 Methods

3.1 Analytical method

When DTM is used for solving differential equations with the boundary conditions at infinity or problems that have highly nonlinear behavior, the outcomes were diverse solutions. Furthermore, power series are ineffective when the independent variable has large values. To address this problem, MDTM has been used for the analytical solution of differential equations, and it is discussed in this section. For this, the following nonlinear initial value problem is considered.

By applying differential transformation theorems on Eqs. (13) and (14), the following recursive relations can be obtained:

$$\begin{aligned}&(k+1)(k+2)V(k+2) + 6\delta(1-\varphi)^{2.5}\sum_{r_2=0}^{k}\sum_{r_1=0}^{r_2}(r_1+1)(r_2-r_1+1)(k-r_2+1)(k-r_2+2)\\ &V(r_1+1)V(r_2-r_1+1)V(k-r_2+2) + \Theta(k) - A\mathrm{Ha}^2(1-\varphi)^{2.5}V(k) - \frac{P}{B}V(k) = 0,\end{aligned} \tag{17}$$

$$\begin{aligned}&\left(1+\frac{4}{3BR_d}\right)(k+1)(k+2)\Theta(k+2) + 2\delta\mathrm{Ec}\,\mathrm{Pr}\sum_{r_3=0}^{k}\sum_{r_2=0}^{r_3}\sum_{r_1=0}^{r_2}(r_1+1)(r_2-r_1+1)(r_3-r_2+1)\\ &(k-r_3+1)V(r_1+1)V(r_2-r_1+1)V(r_3-r_2+1)V(k-r_3+1) + \frac{E_cP_r}{B}(1-\varphi)^{-2.5}\sum_{r=0}^{k}(r+1)(k-r+1)\\ &V(r+1)V(k-r+1) + \frac{\alpha}{B}\Theta(k) = 0,\end{aligned} \tag{18}$$

where $V(k)$ and $\Theta(k)$ are the differential transforms of $u(\eta)$ and $\theta(\eta)$.

The boundary condition's (15–16) differential transform is as follows:

$$V(0) = 0,\ \Theta(0) = \frac{1}{2}, \tag{19}$$

$$\sum_{k=0}^{i} v(k)2^k = 0,\ \sum_{k=0}^{i}\Theta(k)2^k = -\frac{1}{2}, \tag{20}$$

We can consider the following boundary conditions (15–16):

$$v(-1) = 0,\ \theta(-1) = \frac{1}{2}, \tag{21}$$

$$v'(-1) = \lambda,\ \theta'(-1) = \omega, \tag{22}$$

Then, differential transforms of (21–22) are given by

$$V(0) = 0,\ \Theta(0) = \frac{1}{2}, \tag{23}$$

$$V(1) = \lambda,\ \Theta(1) = \omega, \tag{24}$$

Moreover, by substituting Eqs. (23) and (24) into Eqs. (17) and (18) and by the recursive method, we can calculate other values of $V(k)$ and $\Theta(K)$ with the aid of Mathematica 12.3 algorithms.

3.2 Finite difference method

The system of coupled nonlinear ordinary differential Eqs. (13–14) with boundary conditions (15–16) is solved for the flow velocity and temperature using FDM by designing MATLAB and Mathematica programs and then the present graphics are drawn by designing the Excel program. The following linearized form should be applied because of nonlinearity in this system:

$$\begin{aligned}&\frac{\mathrm{d}^2v}{\mathrm{d}\eta^2}\left(1+6(1-\varphi)^{2.5}\left(\frac{\mathrm{d}\bar{v}}{\mathrm{d}\eta}\right)^2\right)\\ &\quad+\theta\left(A\mathrm{Ha}^2(1-\varphi)^{2.5}+\frac{P}{B}\right)v = 0,\end{aligned} \tag{25}$$

$$\left(1+\frac{4}{3BR_d}\right)\frac{\mathrm{d}^2\theta}{\mathrm{d}\eta^2}+\mathrm{Ec}\ \mathrm{Pr}\ \frac{\mathrm{d}\nu}{\mathrm{d}\eta}\left(2\delta\left(\frac{\mathrm{d}\bar{\nu}}{\mathrm{d}\eta}\right)^3+\frac{(1-\varphi)^{-2.5}}{B}\frac{\mathrm{d}\bar{\nu}}{\mathrm{d}\eta}\right)^3+\frac{\alpha}{B}\theta=0, \tag{26}$$

where bar notation denotes the iterated terms that convert Eqs. (13–14) to a linearized one.

By applying Taylor's expansions of the dependent variables about central point for Eqs. (25–26), a system of algebraic equations [33] is obtained:

$$\frac{\mathrm{d}\nu_i}{\mathrm{d}\eta}=\frac{\nu_{i+1}-\nu_{i-1}}{\Delta}+o(\Delta^2) \tag{27}$$

$$\frac{\mathrm{d}^2\nu_i}{\mathrm{d}\eta^2}=\frac{\nu_{i+1}-2\nu_i+\nu_{i-1}}{\Delta^2}+o(\Delta^2) \tag{28}$$

$$\frac{\mathrm{d}^2\theta_i}{\mathrm{d}\eta^2}=\frac{\theta_{i+1}-2\theta_i+\theta_{i-1}}{\Delta^2}+o(\Delta^2) \tag{29}$$

where $i=1, 2, 3,\ldots, m+1$ and m is the number of subintervals of the finite domain of solution $(-1<\eta<1)$.

3.3 Shooting method

Numerical solutions of the ordinary differential Eqs. (13–14) subject to Neumann boundary conditions (15) and (16) are obtained using classical Runge–Kutta method with shooting techniques and MATLAB package (ode45). The set of coupled nonlinear ordinary differential equations along with boundary conditions have been reduced to a system of simultaneous equations of the first order for the unknowns following the method of superposition in Na [34].

Equations (13)–(14) can be written as follows:

$$z_1^{'}=z_2, \tag{30}$$

$$z_2^{'}=\frac{-z_3+AH_a^2(1-\varphi)^{2.5}z_1+\frac{P}{B}z_1}{1+6\delta(1-\varphi)^{2.5}(z_2)^2} \tag{31}$$

$$z_3^{'}=z_4, \tag{32}$$

$$z_4^{'}=\frac{-2\delta E_cP_r(z_2)^4-\left(\frac{E_cP_r}{B}\right)(1-\varphi)^{-2.5}(z_2)^2-\frac{\alpha}{B}z_3}{\left(1+\frac{4}{3BR_d}\right)} \tag{33}$$

where $z_1=\nu$ and $z_3=\theta$.

The initial conditions are

$$z_1(-1)=0,\ z_2(-1)=i_1,\quad z_3(-1)=\frac{1}{2},\ z_4(-1)=i_2, \tag{34}$$

where i_1 and i_2 are a priori unknowns that must be resolved as part of the solution.

Ode45 integrates the system of differential Eqs. (30–33) with suitable guess values for initial conditions i_1 and i_2. The calculated values of the velocity and temperature profiles are compared with the given boundary conditions.

4 Results

4.1 Discussion

In this paper, MDTM, FDM, and shooting method are applied successfully to find the solution of the radiation effect on MHD flow of Rivlin–Ericksen nanofluid of grade three through porous medium with uniform heat source between two vertical flat plates. Tables and graphical representation of the results are very useful to demonstrate the efficiency and accuracy of MDTM, FDM, and shooting method for the problem stated in this work. In order to ensure that the current results are accurate, we compared these results with the previously published work. The graphs (2–9) (a) and (b) show the effects of ϕ, δ, P, Ha, R_d, Ec, Pr, and α on $V(\eta)$ and $\theta(\eta)$ profiles. Figures 2, 3, 4, and 5a show that an increase in ϕ, α, Ec, and Pr parameters leads to an increase in $V(\eta)$, but Figs. 6, 7, 8, and 9a present that an increase in δ, R_d, Ha, and P parameters leads to a decrease in $V(\eta)$. In addition, Figs. 2, 3, 4, and 5b show that an increase in ϕ, α, Ec, and Pr parameters leads to an increase in $\theta(\eta)$, but Figs. 6, 7, 8, and 9b present that an increase in δ, R_d, Ha, and P parameters leads to a decrease in $\theta(\eta)$. It can also be observed that P and Ha on $\theta(\eta)$ are very little, almost nonexistent (Figs. 8 and 9b).

In addition, Tables 2 and 3 show comparison between MDTM, FDM, and shooting method with GM, LSM, and CM [32]. As can be seen, this approximate analytical and numerical solution is in good agreement with the relevant solutions.

Moreover, Tables 4, 5, 6, and 7 (Nu and HPM [35]) demonstrate a comparison between MDTM, FDM, and shooting technique. This approximate analytical and

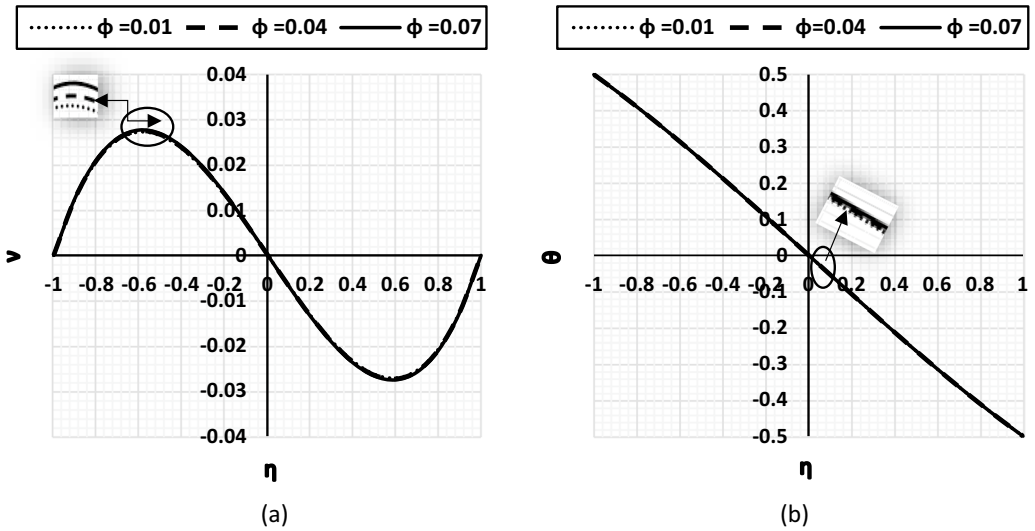

Fig. 2 Result of $V(\eta)$ and $\theta(\eta)$ for various φ when $R_d = 1$, $\delta = 1$, $P = 1$, Ha = 1, Ec = 1, $P_{\mathbf{r}} = 1$, and $\alpha = 1$

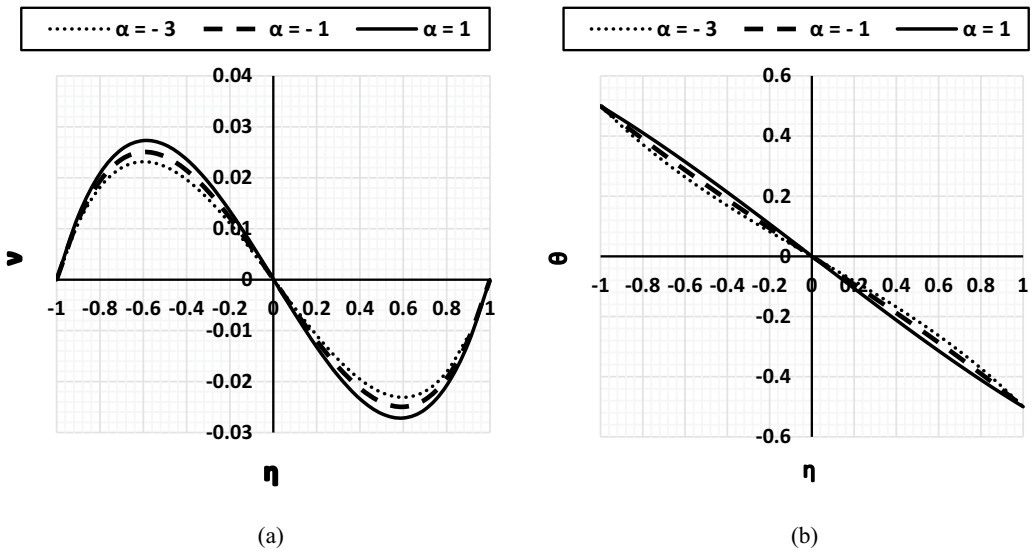

Fig. 3 Result of $V(\eta)$ and $\theta(\eta)$ for various α when $\varphi = 0.01$, $\delta = 1$, $P = 1$, Ha = 1, Ec = 1, Pr = 1, and $R_d = 1$

numerical solution agrees well with the pertinent solutions, as can be seen.

5 Conclusions

In this paper, the radiation effect on MHD flow of Rivlin–Ericksen nanofluid of grade three through porous medium with uniform heat source between two vertical flat plates is studied analytically by MDTM and numerically by FDM and shooting method. Results in graphs and tables for the velocity and temperature profiles are presented and discussed for various parameters φ, δ, P, Ha, R_d, Ec, Pr, and α. Moreover, the results indicate the restraining effects of various parameters on velocity and temperature. Furthermore, comparisons with previously published works are made and showed that the present results have high accuracy and are

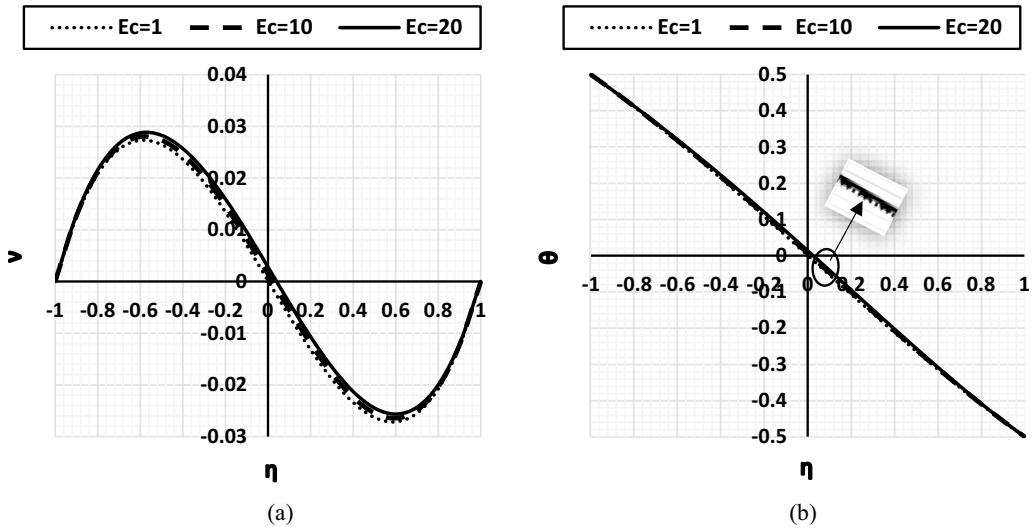

Fig. 4 Result of $V(\eta)$ and $\theta(\eta)$ for various Ec when $\varphi = 0.01$, $\delta = 1$, $P = 1$, Ha $= 1$, $R_d = 1$, Pr $= 1$, and $\alpha = 1$

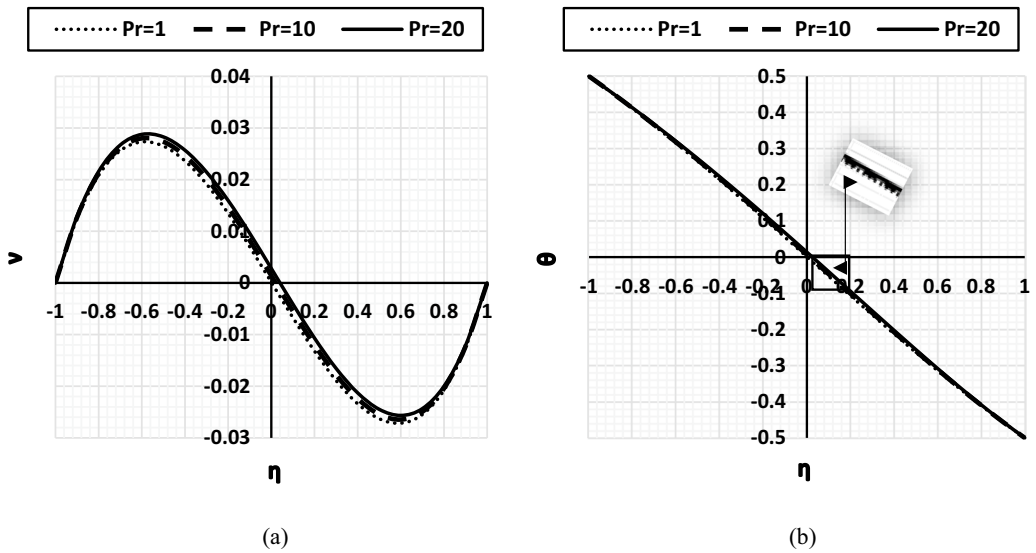

Fig. 5 Result of $V(\eta)$ and $\theta(\eta)$ for various Pr when $\varphi = 0.01$, $\delta = 1$, $P = 1$, Ha $= 1$, Ec $= 1$, $R_d = 1$, and $\alpha = 1$

found to be in good agreement. In particular, results for different parameters are summarized in the next two paragraphs.

- It has been found that the parameters ϕ, α, Ec, and Pr vary directly with velocity $v(\eta)$ and temperature $\theta(\eta)$.
- It has been displayed that the parameters δ, P, Ha, and R_d vary inversely with velocity $v(\eta)$ and temperature $\theta(\eta)$.

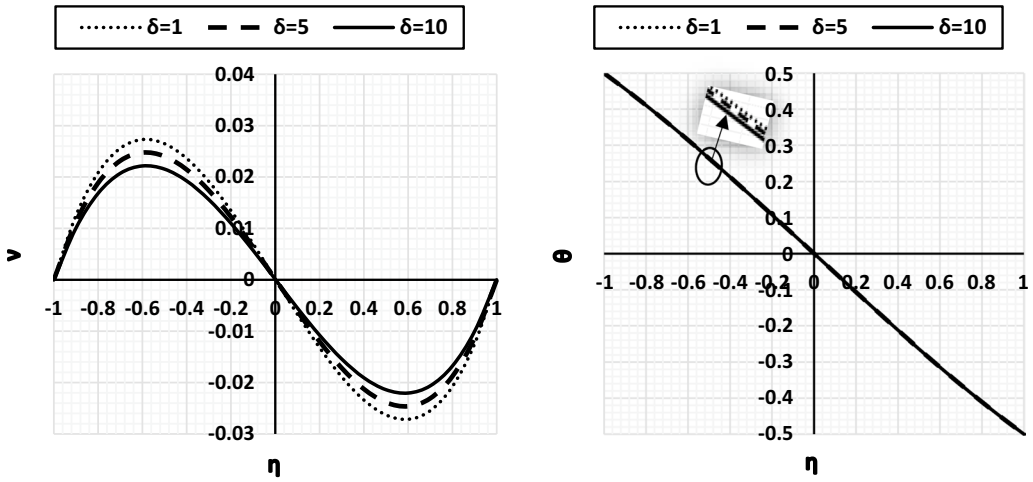

Fig. 6 Result of $V(\eta)$ and $\theta(\eta)$ for various δ when $\varphi = 0.01$, $R_d = 1$, $P = 1$, Ha = 1, Ec = 1, $P_r = 1$, and $\alpha = 1$

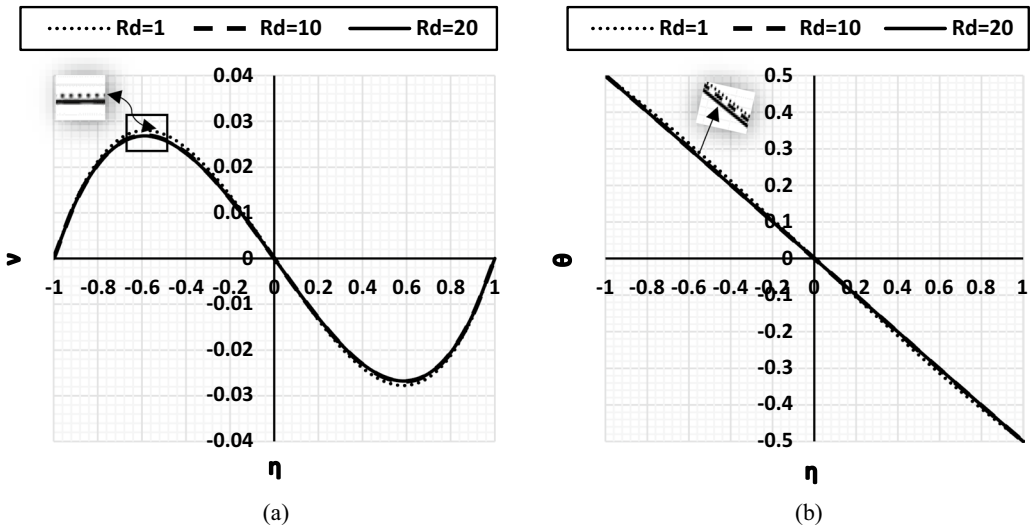

Fig. 7 Result of $V(\eta)$ and $\theta(\eta)$ for various R_d when $\varphi = 0.01$, $\delta = 1$, $P = 1$, Ha = 1, Ec = 1, Pr = 1, and $\alpha = 1$

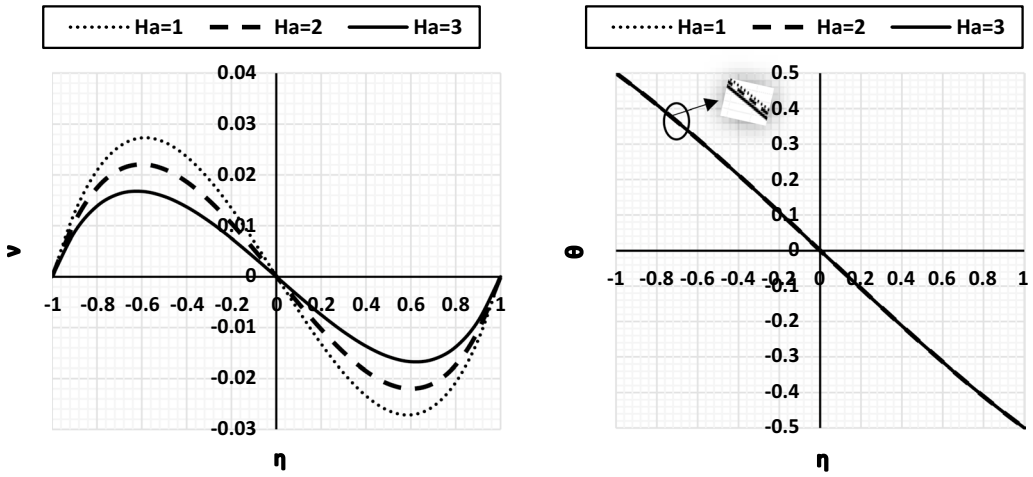

Fig. 8 Result of $V(\eta)$ and $\theta(\eta)$ for various Ha when $\varphi = 0.01$, $\delta = 1$, $P = 1$, $R_d = 1$, Ec = 1, Pr = 1, and $\alpha = 1$

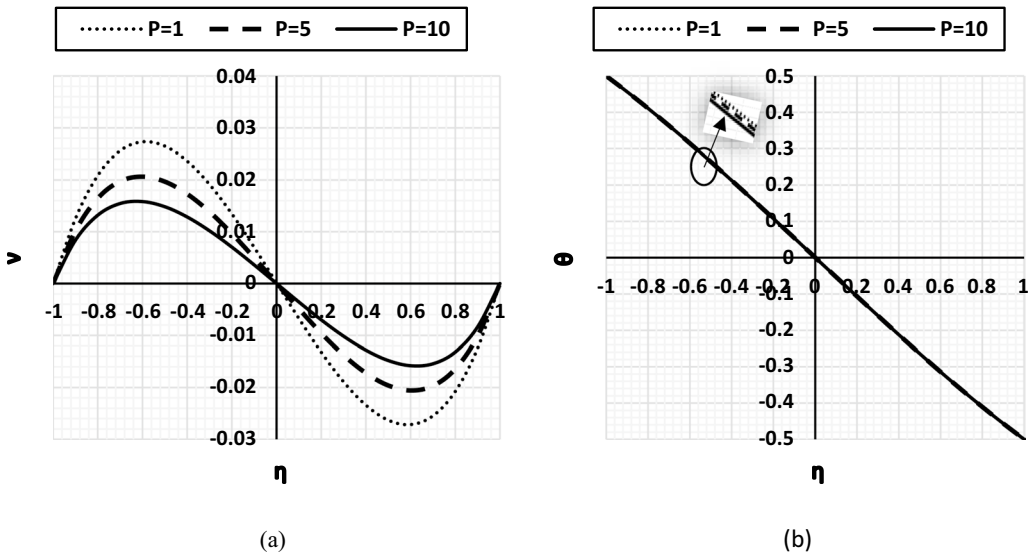

Fig. 9 Result of $V(\eta)$ and $\theta(\eta)$ for various P when $\varphi = 0.01$, $\delta = 1$, $R_d = 1$, Ha = 1, Ec = 1, Pr = 1, and $\alpha = 1$

Table 2 Comparison solution by MDTM, FDM, and shooting method with GM, LSM, and CM [32] for $V(\eta)$ when $\varphi = 0.01$, $\delta = 1$, $P = 0$, $\mathrm{Ha} = 3$, $R_d = 2$, $\mathrm{Ec} = 1$, $\mathrm{Pr} = 6.2$, and $\alpha = 0$

η	Present $v(\eta)$			$v(\eta)$ [32]		
	MDTM	FDM	Shooting method	G.M	L.S.M	C.M
−1	0	0	0	0	0	0
−0.9	0.008927973453246	0.008787225412899	0.008957094	0.007785	0.008539	0.006847
−0.8	0.014223686772939	0.013959477936244	0.014244837	0.013111	0.014381	0.011531
−0.7	0.016769654790264	0.016440045972315	0.016784495	0.016252	0.017827	0.014294
−0.6	0.017266325478027	0.016922743531933	0.017251388	0.017481	0.019175	0.015375
−0.5	0.016255425114184	0.015931229672889	0.016188057	0.017072	0.018726	0.015014
−0.4	0.014150728407177	0.013863775889415	0.014023246	0.015296	0.016779	0.013453
−0.3	0.011268952330109	0.011027308517539	0.011090881	0.012428	0.013633	0.010931
−0.2	0.007857588237348	0.007663635866098	0.007649044	0.008741	0.009589	0.007687
−0.1	0.004116729433862	0.003970101131019	0.003898955	0.004507	0.004945	0.003964
0	0.000217343161713	0.000116424993575	3.9459E06	4.23×10^{-7}	1.54×10^{-6}	1.81×10^{-9}
0.1	−0.003683298028354	−0.003740824702763	−0.003891557	−0.00451	−0.00494	−0.00396
0.2	−0.007427456163251	−0.007444902635067	−0.007643058	−0.00874	−0.00959	−0.00769
0.3	−0.010842771287347	−0.010825560149113	−0.011087014	−0.01243	−0.01363	−0.01093
0.4	−0.013726806197571	−0.013684591023138	−0.014021855	−0.0153	−0.01678	−0.01345
0.5	−0.015828922831118	−0.015779021734224	−0.016189006	−0.01707	−0.01872	−0.01501
0.6	−0.016828099926917	−0.016800520671318	−0.017253911	−0.01748	−0.01917	−0.01537
0.7	−0.016305660627378	−0.016349281399216	−0.016787055	−0.01625	−0.01783	−0.01429
0.8	−0.0137132512402211	−0.013900167871314	−0.014244981	−0.01311	−0.01438	−0.01153
0.9	−0.0083405628843889	−0.008758254914885	−0.008951319	−0.00778	−0.00854	−0.00685
1	0.0007030694820217	0	0	0	0	0

Table 3 Comparison solution by MDTM, FDM, and shooting method with GM, LSM, and CM [32]) for $\theta(\eta)$ when $\varphi=0.01$, $\delta=1$, $P=0$, Ha = 3, $R_d=2$, Ec = 1, Pr = 6.2, and $\alpha=0$

η	Present $\theta(\eta)$			$\theta(\eta)$ [32]		
	MDTM	FDM	Shooting method	G.M	L.S.M	C.M
−1	0.5	0.5	0.5	0.5	0.5	0.5
−0.9	0.45048334393744	0.4500557057	0.449970142	0.449982	0.449947	0.449999
−0.8	0.400767395390827	0.40020133769	0.399959597	0.399969	4.00E-01	0.399998
−0.7	0.350989746391596	0.35039626873	0.349957975	0.349962	0.349892	0.349997
−0.6	0.301201167815963	0.30061028898	0.299961713	0.29996	0.299885	0.299997
−0.5	0.251410810147527	0.25082103146	0.249968222	0.249961	0.24989	0.249997
−0.4	0.201610063585561	0.20101206823	0.199975753	0.199966	0.199905	0.199997
−0.3	0.151784736266043	0.15117151419	0.149983257	0.149973	0.149926	0.149998
−0.2	0.101920941655585	0.10129101917	0.099990246	0.099983	0.099954	0.099998
−0.1	0.052007749159865	0.05136506198	0.049996659	0.049994	0.049985	0.049999
0	0.002038317205475	0.00139048604	2.7177E-06	4.73×10^{-6}	1.74×10^{-5}	2.05×10^{-8}
0.1	−0.04798969711509	−0.04863376327	−0.049991207	−0.04998	−0.04995	−0.05
0.2	−0.09807401948685	−0.09870672228	−0.099984735	−0.09997	−0.09992	−0.10
0.3	−0.14820784031401	−0.14882532079	−0.149977617	−0.14996	−0.14989	−0.15
0.4	−0.19838020932551	−0.19898411506	−0.199969867	−0.19996	−0.19988	−0.20
0.5	−0.24857715789604	−0.24917481927	−0.249961909	−0.24995	−0.24986	−0.25
0.6	−0.29878442328292	−0.29938559613	−0.299954708	−0.29995	−0.29986	−0.30
0.7	−0.3489934561497	−0.34960004659	−0.34994991	−0.34996	−0.34987	−0.35
0.8	−0.3992138754586	−0.39979581311	−0.399949984	−0.39997	−0.3999	−0.40
0.9	−0.44949797889672	−0.44994267864	−0.449958355	−0.44998	−0.44994	−0.45
1	−0.4999868653492	−0.5	−0.5	−0.5	−0.5	−0.5

Table 4 Comparison solution by MDTM, FDM, and shooting method with Nu and HPM [35] for $V(\eta)$ when $\varphi=0.01$, $\delta=1$, $P=0$, Ha = 0, $\frac{1}{R_d}=0$, Ec = 1, Pr = 6.2, and $\alpha=0$

η	Present $v(\eta)$			$v(\eta)$ [35]	
	MDTM	FDM	Shooting method	Nu	HPM
−1	0	0	0.000008625000000	0	−1.00e−12
−0.8	0.0248889137406262	0.025100805859412	0.025678351456000	2.49e-02	0.024978
−0.6	0.0343610151313935	0.034694542987441	0.035179982872000	0.034361	0.034499
−0.4	0.0315996426708186	0.031972343649594	0.032362783968000	0.0316000	0.031771
−0.2	0.0205042979192536	0.020866193989263	0.021116768584000	0.020505	0.020717
0	0.0050363939659476	0.005367924421495	0.005374300000000	0.005037	0.005283
0.2	−0.0109298916536909	−0.010638770093157	−0.01088830874400	−1.09e−02	−1.07e−02
0.4	−0.0234796480160966	−0.023252896625209	−0.02364919452800	−2.35e−02	−2.32e−02
0.6	−0.0285202216294248	−0.028395751318524	−0.02883934383200	−2.85e−02	−2.83e−02
0.8	−0.0218952703866748	−0.021876616709771	−0.02234099241600	−2.19e−02	−2.17e−02
1	1.27761*10^-7	0	0.000013975000000	0	1.00e−12

Table 5 Comparison solution by MDTM, FDM, and shooting method with Nu and HPM [35] for $V(\eta)$ when $\varphi=0.07$, $\delta=2$, $P=0$, Ha $=0$, $\frac{1}{R_d}=0$, Ec $=2$, Pr $=6.2$, and $\alpha=0$

η	Present $v(\eta)$			$v(\eta)$ [35]	
	MDTM	FDM	Shooting method	Nu	HPM
−1	0	0	0.000017360000000	0.000000	2.00e−11
−0.8	0.0263871069970389	0.026756648117180	0.028131952780800	2.64e−02	0.026707
−0.6	0.0377968202181078	0.038456991519952	0.039791286425600	0.037801	0.038229
−0.4	0.0366455592452191	0.037449540554391	0.038657135014400	0.036652	0.037135
−0.2	0.0266332183474780	0.027461728992522	0.028476807859200	0.026641	0.027227
0	0.0116755798181022	0.012471144615492	0.013091000000000	0.011684	0.012360
0.2	−0.0044314126089784	−0.003695940273408	−0.00355835729920	−4.42e−03	−3.73e−03
0.4	−0.0178316240970406	−0.017207382328530	−0.01742024605440	−1.78e−02	−1.72e−02
0.6	−0.0243573107682773	−0.023940881135197	−0.02432671106560	−2.44e−02	−2.37e−02
0.8	0.0196282178526106	−0.019476674321430	−0.01998500942080	−1.96e−02	−1.90e−02
1	3.524349637965*^-7	0	0.000030240000000	0.000000	0.000000

Table 6 Comparison solution by MDTM, FDM, and shooting method with Nu and HPM [35] for $\theta(\eta)$ when $\varphi=0.01$, $\delta=1$, $P=0$, Ha $=0$, $\frac{1}{R_d}=0$, Ec $=1$, Pr $=6.2$, and $\alpha=0$

η	Present $\theta(\eta)$			$\theta(\eta)$ [35]	
	MDTM	FDM	Shooting method	Nu	HPM
−1	0.500000000000000	0.500000000000000	0.500612300000000	0.5	0.5
−0.8	0.4048517213003998	0.404741915710620	0.404681040960000	0.404852	0.404687
−0.6	0.3075705040841343	0.308430072374435	0.308052719840000	0.307571	0.307541
−0.4	0.2100694862476117	0.211064469991446	0.210698745920000	0.210070	0.210225
−0.2	0.1121566516441399	0.112645108561653	0.112462917600000	0.112157	0.112397
0	0.0130337276413045	0.013171988085055	0.013145000000000	0.013034	0.013246
0.2	−0.0877464857138474	−0.087354891438347	−0.08741569744000	−8.77e−02	−8.76e−02
0.4	−0.1899083279925779	−0.188935530008554	−0.18925674336000	−0.189907	−0.189774
0.6	−0.2926661222188964	−0.291569927625565	−0.29220900688000	−0.292665	−0.292458
0.8	−0.3955710872738615	−0.395258084289380	−0.39581308000000	−0.395570	−0.395312
1	−0.5000000187397369	−0.500000000000000	−0.49923570000000	−0.5	−0.5

Table 7 Comparison solution by MDTM, FDM, and shooting method with Nu and HPM [35] for $\theta(\eta)$ when $\varphi=0.07$, $\delta=2$, $P=0$, Ha $=0$, $\frac{1}{R_d}=0$, Ec $=2$, Pr $=6.2$, and $\alpha=0$

η	Present $\theta(\eta)$			$\theta(\eta)$ [35]	
	MDTM	FDM	Shooting method	Nu	HPM
−1	0.500000000000000	0.500000000000000	0.501532200000000	5.00e−01	0.500000
−0.8	0.4122424546865951	0.411231537502520	0.412400824640000	0.412251	0.410966
−0.6	0.3184236211524941	0.319967177782257	0.320214567360000	0.318437	0.317645
−0.4	0.2238523181397247	0.226206920839213	0.226089794880000	0.223868	0.223923
−0.2	0.1285597853705173	0.129950766673386	0.130139604800000	0.128579	0.129006
0	0.0307284125447637	0.031198715284777	0.031893000000000	0.030749	0.030992
0.2	−0.0709204281187916	−0.070049233326614	−0.06928593696000	−7.09e−02	−7.10e−02
0.4	−0.1760391250819469	−0.173793079160787	−0.17377886944000	−0.176022	−0.176076
0.6	−0.282882693412802	−0.280032822217743	−0.28129403232000	−0.282871	−0.282354
0.8	−0.3900682662257274	−0.388768462497480	−0.39044705760000	−0.390062	−0.389033
1	−0.4999999247040331	−0.500000000000000	−0.49834180000000	−0.500000	−0.500000

List of symbols
$2b$: Distance between the plates; g: Gravity; T: Temperature; T_1, T_2: Temperatures at left and right plates, respectively; T_m: Mean temperature; β_3: Rheological material constant; q_r: Radiative heat flux; σ^*: Stephan–Boltzmann constant; K^*: Mean absorption coefficient; ρ_{nf}: Effective density; μ_{nf}: Effective dynamic viscosity; $(\rho C_p)_{nf}$: Heat capacitance; κ_{nf}: Thermal conductivity; φ: Solid volume fraction of the nanoparticles; u: Velocity of fluid; η: Dimensionless variable; v : Dimensionless velocity; θ: Dimensionless temperature; Ec: Eckert number; Pr: Prandtl number; α: Heat source parameter; P: Porosity parameter; Ha^2: Hartmann number; R_d: Radiation parameter; δ: Dimensionless non-Newtonian viscosity; MDTM: Multi-step differential transform method; FDM: Finite difference method.

Acknowledgements
The author thanks all for their help in this study.

Author contributions
The numerical results of the model system are presented using MATLAB, Mathematica, and Excel. The author has read and approved the manuscript.

Funding
There is no source of funding for this study.

Availability of data and materials
Not applicable.

Declarations

Ethics approval and consent to participate
Not applicable.

Consent for publication
Not applicable.

Competing interests
There is no competing interest.

Received: 13 December 2021 Accepted: 3 June 2022
Published online: 15 June 2022

References

1. Soliman HAA (2022) MHD Natural Convection of grade three of non-newtonian fluid flow between two vertical flat plates through porous medium with heat source effect. JES. J Eng Sc
2. Xiang JH, Zhang CL, Zhou C, Liu GY, Zhou W (2018) Heat transfer performance testing of a new type of phase change heat sink for high power light emitting diode. J Cent South Univ 25(7):1708–1716
3. Wang WH, Cheng DL, Liu T, Liu YH (2016) Performance comparison for oil-water heat transfer of circumferential overlap trisection helical baffle heat exchanger. J Cent South Univ 23(10):2720–2727
4. Maghsoudi P, Siavashi M (2019) Application of nanofluid and optimization of pore size arrangement of heterogeneous porous media to enhance mixed convection inside a two-sided lid-driven cavity. J Therm Anal Calorim 135(2):947–961
5. Mosayebidorcheh S, Rahimi-Gorji M, Ganji DD, Moayebidorcheh T, Pourmehran O, Biglarian M (2017) Transient thermal behavior of radial fins of rectangular, triangular and hyperbolic profiles with temperature-dependent properties using DTM-FDM. J Cent South Univ 24(3):675–682
6. Xie N, Jiang CW, He YH, Yao M (2017) Lattice Boltzmann method for thermomagnetic convection of paramagnetic fluid in square cavity under a magnetic quadrupole field. J Cent South Univ 24(5):1174–1182
7. Sheikholeslami M (2018) CuO-water nanofluid flow due to magnetic field inside a porous media considering Brownian motion. J Mol Liq 249:921–929
8. Sheikholeslami M, Jafaryar M, Saleem S, Li Z, Shafee A, Jiang Y (2018) Nanofluid heat transfer augmentation and exergy loss inside a pipe equipped with innovative turbulators. Int J Heat Mass Transf 126:156–163
9. Feng JS, Dong H, Gao JY, Liu JY, Liang K (2017) Theoretical and experimental investigation on vertical tank technology for sinter waste heat recovery. J Cent South Univ 24(10):2281–2287
10. Ahmed A, Nadeem S (2017) Biomathematical study of time-dependent flow of a Carreau nanofluid through inclined catheterized arteries with overlapping stenosis. J Cent South Univ 24(11):2725–2744
11. Sheikholeslami M (2018) Influence of magnetic field on Al_2O_3-H_2O nanofluid forced convection heat transfer in a porous lid driven cavity with hot sphere obstacle by means of LBM. J Mol Liq 263:472–488
12. Sheikholeslami M, Rokni HB (2017) Numerical modeling of nanofluid natural convection in a semi annulus in existence of Lorentz force. Comput Methods Appl Mech Eng 317:419–430
13. Sheikholeslami M, Vajravelu KJAM (2017) Nanofluid flow and heat transfer in a cavity with variable magnetic field. Appl Math Comput 298:272–282
14. Majid S, Mohammad J (2017) Optimal selection of annulus radius ratio to enhance heat transfer with minimum entropy generation in developing laminar forced convection of Water-Al 2 O 3 nanofluid flow. J Cent South Univ 24(8):1850–1865
15. Dogonchi AS, Divsalar K, Ganji DD (2016) Flow and heat transfer of MHD nanofluid between parallel plates in the presence of thermal radiation. Comput Methods Appl Mech Eng 310:58–76
16. Dogonchi AS, Ganji DD (2016) Thermal radiation effect on the Nano-fluid buoyancy flow and heat transfer over a stretching sheet considering Brownian motion. J Mol Liq 223:521–527
17. Dogonchi AS, Ganji DD (2017) Impact of Cattaneo–Christov heat flux on MHD nanofluid flow and heat transfer between parallel plates considering thermal radiation effect. J Taiwan Inst Chem Eng 80:52–63
18. Chamkha AJ (1994) Flow of non-newtonian particulate suspension with a compressible particle phase. Mech Res Commun 21(6):645–654
19. Ellahi R, Raza M, Vafai K (2012) Series solutions of non-Newtonian nanofluids with Reynolds' model and Vogel's model by means of the homotopy analysis method. Math Comput Model 55(7–8):1876–1891
20. Youssri YH, Abd-Elhameed WM, Sayed SM (2022) Generalized lucas tau method for the numerical treatment of the one and two-dimensional partial differential heat equation. J Funct Spaces
21. Atta AG, Moatimid GM, Youssri YH (2020) Generalized Fibonacci operational tau algorithm for fractional Bagley–Torvik equation. Prog Fract Differ Appl 6(3):215–224
22. Chen HT, Chen COK (1988) Free convection flow of non-Newtonian fluids along a vertical plate embedded in a porous medium
23. Domairry D, Sheikholeslami M, Ashorynejad HR, Gorla RSR, Khani M (2011) Natural convection flow of a non-Newtonian nanofluid between two vertical flat plates. Proc Inst Mech Eng, Part N: J Nanoeng Nanosyst 225(3):115–122
24. Pittman JFT, Richardson JF, Sherrard CP (1999) An experimental study of heat transfers by laminar natural convection between an electrically-heated vertical plate and both Newtonian and non-Newtonian fluids. Int J Heat Mass Transf 42(4):657–671
25. Hatami M, Ganji DD (2014) Natural convection of sodium alginate (SA) non-Newtonian nanofluid flow between two vertical flat plates by analytical and numerical methods. Case Stud Therm Eng 2:14–22
26. Ternik P, Rudolf R (2013) Laminar natural convection of non-Newtonian nanofluids in a square enclosure with differentially heated side walls. Int J Simul Model 12(1):5–16
27. Rajagopal KR, Na TY (1985) Natural convection flow of a non-Newtonian fluid between two vertical flat plates. Acta Mech 54(3):239–246
28. Aminossadati SM, Ghasemi B (2009) Natural convection cooling of a localised heat source at the bottom of a nanofluid-filled enclosure. Eur J Mech-B/Fluids 28(5):630–640
29. Raptis A (1998) Radiation and free convection flow through a porous medium. Int Commun Heat Mass Transfer 25(2):289–295
30. Ozisik MN (1973) Radiative transfer and interactions with conduction and convection (Book—Radiative transfer and interactions with conduction and convection). Wiley-Interscience, New York, p 587
31. Maxwell JC (1873) A treatise on electricity and magnetism (Vol. 1). Clarendon Press
32. Maghsoudi P, Shahriari G, Rasam H, Sadeghi S (2019) Flow and natural convection heat transfer characteristics of non-Newtonian nanofluid flow bounded by two infinite vertical flat plates in presence of magnetic

field and thermal radiation using Galerkin method. J Cent South Univ 26(5):1294–1305
33. Smith GD, Smith GD, Smith GDS (1985) Numerical solution of partial differential equations: finite difference methods. Oxford university press
34. Na T (1979) Computational methods in engineering boundary value problems. Academic Press, Inc. Mathematics in Science and Engineering, New York, p 145
35. Gholinia M, Ganji DD, Poorfallah M, Gholinia S (2016) Analytical and numerical method in the free convection flow of pure water non-newtonian nano fluid between two parallel perpendicular flat plates. Innov Ener Res 5(142):2

Publisher's Note